Supporting Information

Gregor et al. 10.1073/pnas.1715946115

SI Materials and Methods

Cloning and Mutagenesis. The vector pGEX(−) was generated by PCR of pGEX-6P-1 with the primers pGEX(−) BamHI fwd/pGEX(−) BamHI rev (Table S1). The PCR product was digested with DpnI to remove template DNA and then, gel-purified. Subsequently, the obtained DNA fragment was digested with BamHI and ligated without an insert to obtain pGEX(−). pQE(−) was generated from pQE30 in an analogous way using the primers pQE(−) BamHI fwd/pQE(−) BamHI rev.

luxCDABE was amplified with the primers luxC BamHI fwd/luxE SalI rev and cloned into pGEX-6P-1 and pGEX(−) with BamHI and SalI. The *fre* and *frp* genes were introduced behind *luxE* between the SalI and NotI restriction sites after PCR with primers fre SalI fwd/fre NotI rev and frp SalI fwd/frp NotI rev, respectively. Second copies of *luxA*, *luxAB*, *luxCD*, and *luxE* were also cloned between the SalI and NotI restriction sites using the PCR primers luxA SalI fwd/luxA NotI rev, luxA SalI fwd/luxB NotI rev, luxC SalI fwd/luxD NotI rev, and luxE SalI fwd/luxE NotI rev, respectively.

For error-prone PCRs, an EcoRI restriction site was introduced in front of *luxA* by PCR of the whole plasmid *luxCDABE+frp* pGEX(−) with the primers luxA EcoRI fwd/linker luxDA EcoRI rev, digesting the PCR product with DpnI and EcoRI, and ligation without an insert. Similarly, an NcoI restriction site behind *luxB* was introduced using the primers linker luxBE NcoI fwd/luxB NcoI rev. Error-prone PCRs were performed with the following primers.

luxAB: EP luxAB EcoRI fwd/EP luxAB NcoI rev

luxCD: EP luxCD BamHI fwd/EP luxCD EcoRI rev

luxE: EP luxE NcoI fwd/EP luxE SalI rev

frp: frp SalI fwd/frp NotI rev

Twenty-five PCR cycles were performed with $MnCl_2$ concentrations ranging from 50 to 150 μM. The PCR products were gel-purified, digested with the enzymes indicated in the primer names, and ligated back into the *lux* pGEX(−) vector.

For the construction of *ilux* pGEX(−) containing EYFP-*iluxA*, *iluxA*-EYFP, EYFP-*iluxB*, and *iluxB*-EYFP, respectively, with the EYFP separated by a glycine-serine linker (GS), the *luxAB*+EYFP inserts were assembled by PCR of the following overlapping fragments generated in a previous PCR step with the indicated primers.

EYFP-*iluxA*: EYFP: primers EYFP EcoRI fwd/EYFP overlap luxA rev; *iluxAB*: primers luxA overlap EYFP fwd/EP luxAB NcoI rev; complete insert EYFP+*iluxAB*: primers EYFP EcoRI fwd/EP luxAB NcoI rev

iluxA-EYFP: *iluxA*: primers EP luxAB EcoRI fwd/luxA overlap luxA-EYFP rev; EYFP: primers EYFP fwd/EYFP rev; *iluxB*: primers luxB overlap luxA-EYFP fwd/EP luxAB NcoI rev; complete insert *iluxA*+EYFP+*iluxB*: primers EP luxAB EcoRI fwd/EP luxAB NcoI rev

EYFP-*iluxB*: *iluxA*: primers EP luxAB EcoRI fwd/luxA overlap EYFP-luxB rev; EYFP: primers EYFP fwd/EYFP rev; *iluxB*: primers luxB overlap EYFP-luxB fwd/EP luxAB NcoI rev; complete insert *iluxA*+EYFP+*iluxB*: primers EP luxAB EcoRI fwd/EP luxAB NcoI rev

iluxB-EYFP: *iluxAB*: primers EP luxAB EcoRI fwd/luxB overlap EYFP rev; EYFP: primers EYFP fwd/EYFP NcoI rev; complete insert *iluxAB*+EYFP: primers EP luxAB EcoRI fwd/EYFP NcoI rev

The resulting *luxAB*+EYFP inserts were cloned into *ilux* pGEX(−) with EcoRI and NcoI.

A His tag with a GS was introduced at the indicated proteins in *luxCDABE+frp* and *ilux* pGEX(−) by PCR of the following fragments and subsequent cloning into the original vector with the restriction enzymes given in the primer names.

luxB-His: *luxAB*, primers EP luxAB EcoRI fwd/luxB-His NcoI rev

His-*luxC*: *luxCD*, primers His-luxC BamHI fwd/EP luxCD EcoRI rev

luxD-His: *luxCD*, primers EP luxCD BamHI fwd/luxD-His EcoRI rev

luxE-His: *luxE*, primers EP luxE NcoI fwd/luxE-His SalI rev

His-*frp*: *frp*, primers His-frp SalI fwd/frp NotI rev or ifrp NotI rev, respectively

frp-His: *frp*, primers frp SalI fwd/frp-His NotI rev or ifrp-His NotI rev, respectively

For the other constructs, two overlapping fragments were used to assemble the complete insert.

luxA-His: *luxA*: primers EP luxAB EcoRI fwd/luxA overlap luxA-His rev; *luxB*: primers luxB overlap luxA-His fwd/EP luxAB NcoI rev; complete insert *luxAB*: primers EP luxAB EcoRI fwd/EP luxAB NcoI

luxC-His: *luxC*: primers EP luxCD BamHI fwd/luxC overlap luxC-His rev; *luxD*: primers luxD overlap luxC-His fwd/EP luxCD EcoRI rev; complete insert *luxCD*: primers EP luxCD BamHI fwd/EP luxCD EcoRI rev

FLuc was amplified with the primers FLuc BamHI fwd/FLuc SalI rev and cloned into pQE(−) between the BamHI and SalI restriction sites; *luxCDABE WT* was cloned from pGEX(−) into pQE(−) by excision of the complete insert with BamHI and SalI and ligation into pQE(−) digested with the same enzymes. For cloning of *ilux* and *ilux* containing EYFP-tagged *luxB* from pGEX(−) into pQE(−), an XmaI restriction site behind the *frp* gene in pGEX(−) was introduced by PCR of *frp* with the primers frp SalI fwd/frp XmaI NotI rev and cloning the PCR product back into the vector with SalI and NotI. Subsequently, the complete *ilux* operons were cut out with BamHI and XmaI and ligated into pQE(−) digested with the same enzymes.

For replacement of the ampicillin resistance gene in pQE(−) with kanamycin resistance, the kanamycin resistance gene was amplified with the primers KanR SpeI fwd/KanR AscI rev and ligated into pQE(−) amplified with the primers pQE(−) AscI fwd/pQE(−) SpeI rev after digestion with the indicated enzymes; *ilux* was subsequently cloned into pQE(−) containing the kanamycin resistance gene with BamHI and XmaI as described above.

To construct *ilux*+QUEEN-2m pQE(−), *frp* was amplified from *ilux* pGEX(−) with the primers frp SalI fwd/frp AscI XmaI NotI rev and cloned back into the same vector with SalI and NotI. Subsequently, QUEEN-2m was amplified with the primers QUEEN-2m AscI fwd/QUEEN-2m XmaI rev and cloned into the resulting plasmid with AscI and XmaI. Finally, the complete *ilux*+QUEEN-2m insert was cloned from pGEX(−) into pQE(−) by excision with BamHI and XmaI and ligation into pQE(−) digested with the same enzymes.

Measurement of Temperature Curves. To compare the brightness of *luxCDABE* WT and *ilux* at different temperatures, *Escherichia coli*

DH5α cells containing *luxCDABE* WT or *ilux* pGEX(−) were grown on LB agar plates at 37 °C. The following day, cells were resuspended in PBS supplemented with 20 mM D-glucose. The cell suspension was equilibrated to the indicated temperature in a thermocycler (Biometra) and imaged with a PCO Sensicam camera (LaVision). Freshly diluted cell suspension was used for each measurement.

Measurement of Bioluminescence Spectra. *E. coli* Top10 cells expressing *luxCDABE WT* or *ilux* from the vector pQE(−) grown on LB agar plates at 37 °C were resuspended in PBS supplemented with 20 mM D-glucose. Bioluminescence emission of the cell suspension was recorded at room temperature with a Varian Cary Eclipse fluorescence spectrophotometer. To increase the signal-to-noise ratio, 100 measurements were averaged, and the resulting spectra were smoothed by replacing the signal at each data point i by the average of data points i − 1 to i + 1. For baseline correction, the averaged signal between 750 and 800 nm was subtracted.

Western Blot Analysis. DH5α cells expressing *luxCDABE+frp* WT and *ilux* with His-tagged versions of the *lux* proteins from pGEX(−) were grown on LB agar plates at 37 °C. The following day, cells were resuspended in 1× SDS/PAGE loading buffer and heated to 95 °C for 5 min. Lysates were separated on 10% acrylamide gels containing 0.1% SDS at a constant current of 25 mA per gel. Subsequently, proteins were transferred onto nitrocellulose membranes by tank blotting overnight using a constant current of 75 mA per gel. For detection of His-tagged proteins, a Penta-His antibody (Qiagen) was used at a dilution of 1:500 according to the manufacturer's directions. DnaK was detected by anti-DnaK (8E2/2; Enzo Life Sciences) at a dilution of 1:5,000. Both primary antibodies were detected with a secondary HRP-coupled anti-mouse antibody (Dianova). The chemiluminescence was imaged using Western Lightning Plus-ECL solution (Perkin-Elmer) with an Amersham Imager 600 (GE Healthcare).

After subtraction of background, the His signal of each clone was normalized to the corresponding DnaK signal to correct for variations in the amount of loaded sample. Ten clones of each construct were averaged. The values obtained for His-tagged *ilux* proteins were normalized to the corresponding His-tagged *luxCDABE+frp WT* construct.

Imaging. Screening for brighter variants was performed with *E. coli* DH5α cells expressing *lux* proteins from pGEX(−). Cells were grown on LB agar plates containing 50 μg/mL ampicillin (AppliChem) at 37 °C overnight and imaged at 37 °C with a PCO Sensicam camera (LaVision). The brightest clones were selected for the next cycle of mutagenesis.

For comparisons of brightness on agar plates, *E. coli* DH5α colonies expressing the indicated operons from the vector pGEX(−) were spread out onto new LB agar plates containing 50 μg/mL ampicillin and grown overnight at 37 °C. For each clone, the brightness from three different areas was averaged.

For single-cell imaging, *E. coli* Top10 cells expressing the indicated genes from the vector pQE(−) were grown overnight at 37 °C on LB agar plates containing 50 μg/mL ampicillin. Cells from agar plates were resuspended in water; 1 μL of the suspension was placed on a coverslip, covered with an agar pad cut from an LB agar plate, and immediately used for imaging. Agar pads contained 50 μg/mL ampicillin and in addition, 100 μg/mL kanamycin (AppliChem) or 100 μg/mL timentin (TOKU-E) where indicated. For imaging of FLuc, the agar pad additionally contained D-Luciferin at a concentration of 1 mg/mL.

Imaging was performed with a custom-built microscopy setup (Fig. S9). An electron multiplying charge-coupled device (EMCCD) camera (iXon DU860; Andor) was used for detection. The camera sensor was cooled to −93 °C. Readout was performed in kinetics mode using a vertical shift speed of 0.1 μs per pixel and a horizontal readout speed of 1 MHz. The preamplification gain was set to five, and the electron magnification (EM) gain was set to 300 (Real EM gain mode). The effective pixel size of the camera was 120 nm. Two lasers (405 and 491 nm) were available for excitation of fluorescence. The 405-nm laser (PhoxX 405–60; Omicron or DL 100; Toptica) was used to select and focus the cells. The 491-nm laser (Calypso 50 mW; Cobolt) was used for excitation of *luxB*-EYFP and QUEEN-2m. The lasers were focused into the back focal plane of the objective lens, resulting in an illumination area in the sample of about 20 μm in diameter. The utilized laser powers in the back focal plane of the objective were ∼0.3 and ∼15 μW for the 405- and 491-nm lasers, respectively. Fluorescence images were scaled to the minimum and maximum pixel values.

For cells expressing FLuc, samples were prepared with blue fluorescent microspheres (Molecular Probes) with a diameter of 1.0 μm and excitation and emission maxima of 365 and 415 nm, respectively. This allowed focusing of the sample, despite the absence of cellular fluorescence. Excitation was performed with the 405-nm laser and an additional fluorescence filter (D470/40×) in the detection path.

Light from the sample was collected with an HC PL APO 100×/1.40–0.70 OIL CS oil immersion objective lens (Leica). The light was directed to the camera using dielectric mirrors (BB1-E02; Thorlabs), a dichroitic beam splitter (ZT405rdc; Chroma), and a detection filter (BrightLine FF01-842/SP; Semrock) to block light from the focus lock system. For imaging of *luxB*-EYFP, a fluorescence filter (HQ 520/40 M) was inserted into the detection path. The first mirror after the objective lens was a backside-polished version (BB1-E02P; Thorlabs) to allow in- and outcoupling of 980-nm light for the focus lock system. Focusing onto the camera was performed with an achromatic lens with a focal length of f = 400 mm and VIS coating (Qioptiq), resulting in an effective pixel size on the camera of 120 nm. Measurement control and data acquisition were performed with self-written Python programs.

To keep the sample in focus during long-term imaging, a custom-built focus lock was used. The focus lock system measured the axial position of the sample by measuring the position of a laser beam total internally reflected (TIR) at the coverslip–agar interface. For this purpose, a 980-nm laser (SPL-980-15-9-PD; Roithner Lasertechnik) beam was focused off-center into the back focal plane of the objective lens. The TIR signal was detected by a position-sensitive diode. A feedback loop written in Python calculated the necessary shift of the objective to compensate for drifts of the focal plane. The axial position of the objective lens was updated every 100 ms by commanding the objective positioner piezo (MIPOS 100 PL CAP; piezosystem Jena).

To filter out bright pixels due to cosmic radiation, the value of pixels above a brightness threshold was replaced by the average of the same pixel in the previous and following images. Unless otherwise stated, the average background signal from an image taken with the same exposure time without a sample was subtracted.

Calibration of camera pixel values to detected photons was performed by measuring the mean and variance of the pixel values of a uniformly illuminated camera sensor chip for several exposure times. Assuming shot noise for conditions where background counts are negligible, variance and mean of the pixel values N_{ADC} are proportional to each other:

$$\mathrm{var}(N_{ADC}) \propto 2 \cdot \alpha \cdot \mathrm{mean}(N_{ADC}).$$

The proportionality factor α is given by the analog-to-digital converter (ADC) counts per photoelectron and can be obtained by a linear fit to the data. The factor 2 accounts for the excess noise factor of 1.41 of an EMCCD camera. The mean of the camera count offset μ_{offset} was obtained from camera images without illumination. Finally, the conversion of camera ADC counts N_{ADC} to photons N_{photon} was performed by

$$N_{\mathrm{photon}} = \alpha^{-1}\left(N_{ADC} - \mu_{\mathrm{offset}}\right)$$

with the definitions given above.

>iluxC

MTKKISFIITGQVEIFPESDDLVQSINFGDNSVYLPILNDSHVKNIIDCNGNNELRLHDIVNFLYTVGQRWKNDEYSR
RRTYIRDLKKYMGYSEEMAKLEANWISMILCSKGGLYDVVENELGSRHIMDEWLPQDESYVRAFPKGKSVHLLA
GNVPLSGIMSILRAILTKNQCIIKTSSTDPFTANALALSFIDVDPNHPITRSLSVIYWPHQGDTSLAKEIMRHADVIVA
WGGPDAINWAVEHAPSYADVIKFGPKKSLCIIDNPVDLTSAATGAAHDVCFYDQRACFSAQNIYYMGNHYEEFKL
ALIEKLNLYAHILPNAKKDFDEKAAYSLVQKESLFAGLKVEVDIHQRWTIIESDAGVEFNQPLGRCVYLHHVDNIEQI
LPYVQKNKTQTISIFPWESSFKYRDALALKGAERIVEAGMNNIFRVGGSHDGMRPLQRLVTYISHERPSNYTAKDV
AVEIEQTRFLEEDKFLVFVP

>iluxD

MENESKYKTIDHVICVEGNKKIHVWETLPEENSPKRKNAIIIASGFARRMDHFAGLAEYLSRNGFHVIRYDSLHHV
GLSSGTIDEFTMSIGKQSLLAVVDWLTTRKINNFGMLASSLSARIAYASLSEINASFLITAVGVVNLRYSLERALGFD
YLSLPINELPNNLDFEGHKLGAEVFARDCLDFGWEDLASTINNMMYLDIPFIAFTANNDNWVKQDEVITLLSNIRSN
RCKIYSLLGSSHDLSENLVVLRNFYQSVTKAAIAMDNDHLDIDVDITEPSFEHLTIATVNERRMRIEIENQAISLS

>iluxA

MKFGNFLLTYQPPQFSQTEVMERLVKLGRISEECGFDTVWLLEHHFTEFGLLGNPYVAAAYLLGATKKLNVGTAA
IVLPTAHPVRQLEDVNLLDQMSKGRFRFGICRGLYNKDFRVFGADMNNSRALAECWYGLIKNGMTEGYMEADNE
HIKFHKVKVNPAAYSRGGAPVYVVAESAATTEWAAQFGLPMILSWIINTNEKKAQLELYNEVAQEYGHDIHNIDHC
LSYITSVDHDSIKAKEICRKFLGHWYDSYVNATTIFDDSDQTRGYDFNKGQWRDFVLKGHKDTNRRIDYSYEINPV
GTPQECIDIIQKDIDATGISNICCGFEANGTVDEIIASMKLFQSDVMPFLKEKQRSLLY

>iluxB

MKFGLFFLNFINPTTVQEQSIVRMQEITEYVDKLNFEQILVYENHFSDNGVVGAPLTVSGFLLGLTEKIKIGSLNHIIT
THHPVRIAEEACLLDQLSEGRFILGFSDCEKKDEMHFFNRPAEYQQQLFEECYEIINDALTTGYCNPDNDFYSFPK
ISVNPHAYTPGGPRKYVTATSHHIVEWAAKKGIPLIFKWDDSNDVRYEYAERYKAVADKYDVDLSEIDHQLMILVN
YNEDSNKAKQETRAFISDYVLEMHPNEDFENKLEEIIAENAVGNYTECITAAKLAIEKCGAKSVLLSFEPMNDLMS
QKNVINIVDDNIKKYHMEYT

>iluxE

MTSYVDKQEITASSEIDDLIFSSDPLVWSYDEQEKIRKKLVLDAFRNHYKHCREYRHYCQAHKVDDNITEIDDIPVF
PTSVFKFTRLLTSQENEIESWFTSSGTNGLKSQVARDRLSIERLLGSVSYGMKYVGSWFDHQIELVNLGPDRFNA
HNIWFKYVMSLVELLYPTTFTVTEERIDFVKTLNSLERIKNQGKDLCLIGSPYFIYLLCHYMKDKKISFSGDKSLYIIT
GGGWKSYEKESLKRDDFNHLLFDTFNLSDISQIRDIFNQVELNTCFFEDEMQRKHVPPWVYARALDPETLKPVPD
GTPGLMSYMDASATSYPAFIVTDDVGIISREYGKYPGVLVEILRRVNTRTQKGCALSLTEAFDS

>ilux frp

MVKIQPIPTTSQGSLFIMNSTIETILGHRSIRKFTSEPIASEQLQTILQSGLAASSSSMLQVVSIIRVTDTEKRKLLAQY
AGNQTYVESAAEFLVFCIDYQRHATINPDVQADFTELTLIGAVDSGIMAQNCLLAAESMGLGGVYIGGLRNSAAQV
DELLGLPKNTAILFGMCLGHPDQSPETKPRLPAHVIVHENQYQALNIDDVQAYDKTLQEYYASRTSNQKQSVWS
QETAGKLAGESLPHILPYLNSKGLARR

Fig. S1. Amino acid sequences of the *ilux* proteins.

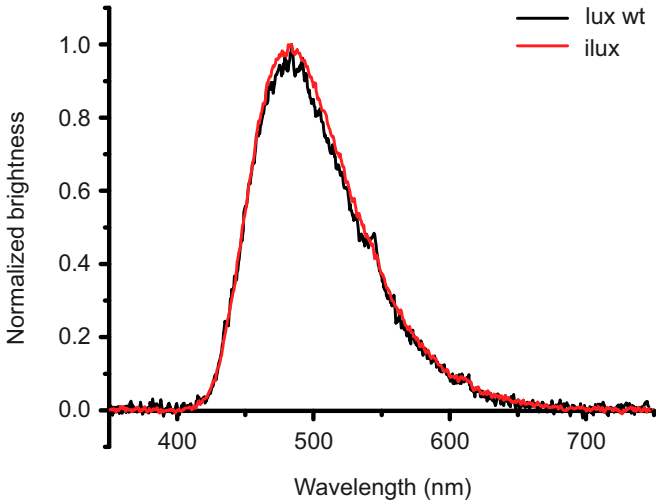

Fig. S2. Bioluminescence spectra of *luxCDABE WT* and *ilux*. Emission of *E. coli* Top10 cells expressing *luxCDABE WT* or *ilux* from the vector pQE(–) was recorded in suspension at room temperature.

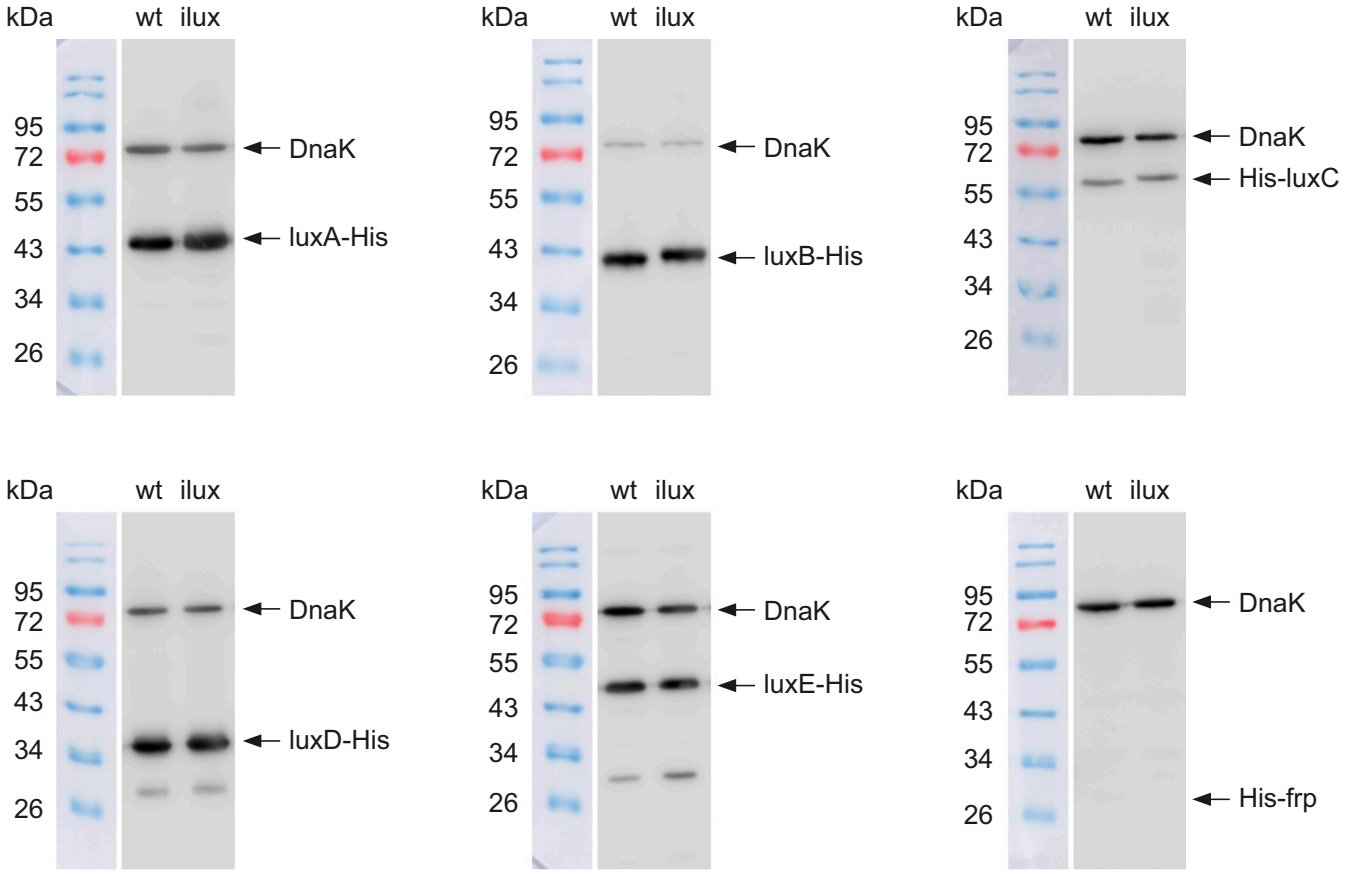

Fig. S3. Western blots of His-tagged *lux* proteins. Lysates of *E. coli* DH5α cells expressing *luxCDABE+frp WT* or *ilux* from the vector pGEX(–) with a His tag at *luxA*, *luxB*, *luxC*, *luxD*, *luxE*, or *frp* were analyzed by SDS/PAGE followed by Western blotting. Expression of the His-tagged proteins was quantified using an anti–Penta-His antibody and anti-DnaK to normalize the His signal to the housekeeping protein DnaK; 1 of 10 clones for each construct is exemplarily shown. The following protein sizes are expected: DnaK: ~70 kDa; *luxA*-His: 42 kDa; *luxB*-His: 39 kDa; His-*luxC*: 56 kDa; *luxD*-His: 36 kDa; *luxE*-His: 44 kDa; and His-*frp*: 28 kDa.

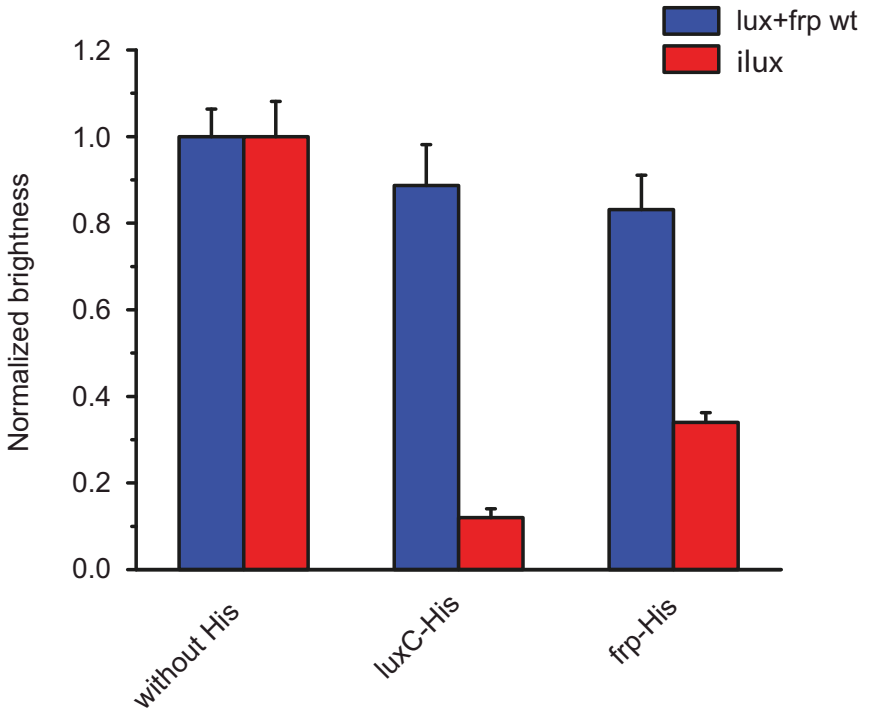

Fig. S4. Brightness of *luxCDABE+frp WT* and *ilux* with *luxC*-His and *frp*-His; *luxCDABE+frp WT* and *ilux* containing a C-terminal His tag at *luxC* and *frp* were expressed from the vector pGEX(–) in *E. coli* DH5α cells on LB agar plates at 37 °C. Plates were imaged at 37 °C. The signal was normalized to the corresponding nontagged *lux* operon. Error bars represent SDs of 10 different clones.

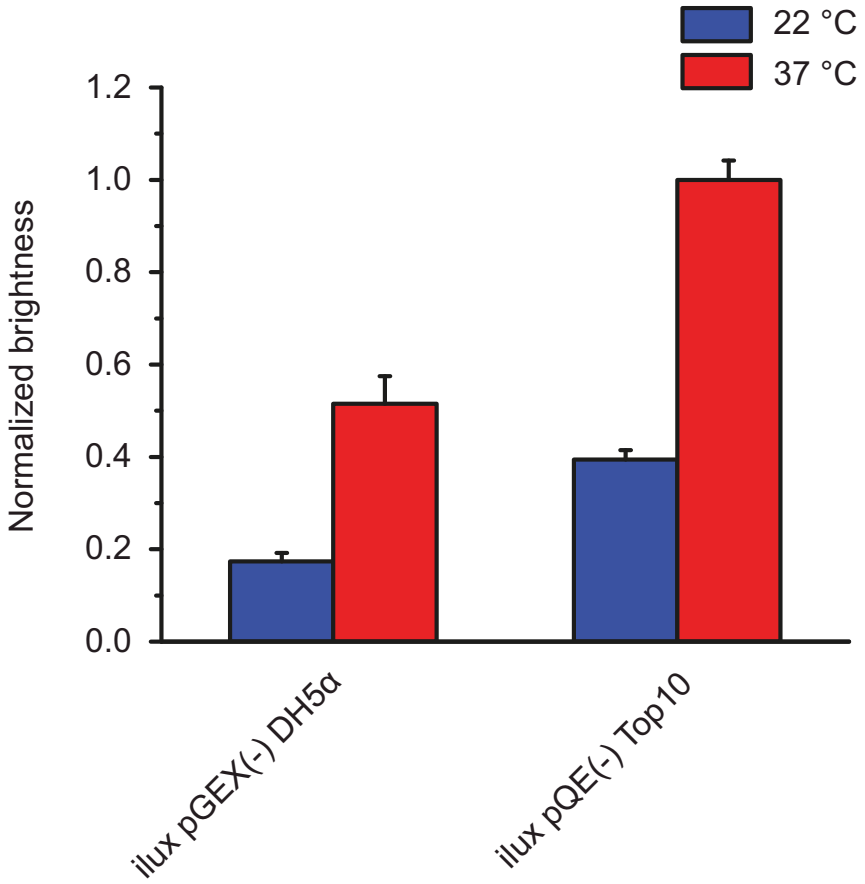

Fig. S5. Brightness of *ilux* in *E. coli* DH5α and Top10 cells. *E. coli* DH5α cells expressing *ilux* from the vector pGEX(–) and *E. coli* Top10 cells expressing *ilux* from the vector pQE(–) were grown on LB agar plates at 37 °C. Plates were imaged at 37 °C and 22 °C. Error bars represent SDs of four different clones.

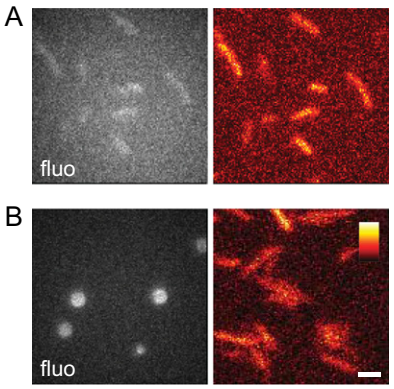

Fig. S6. Scaled images of Fig. 4 *B* and *D*. *A* and *B* represent the images from Fig. 4*B* (Top10 cells expressing *luxCDABE WT*) and Fig. 4*D* (Top10 cells expressing FLuc), respectively, scaled to the minimum and maximum pixel values of each image. Fluo, fluorescence. (Scale bar: 2 μm.)

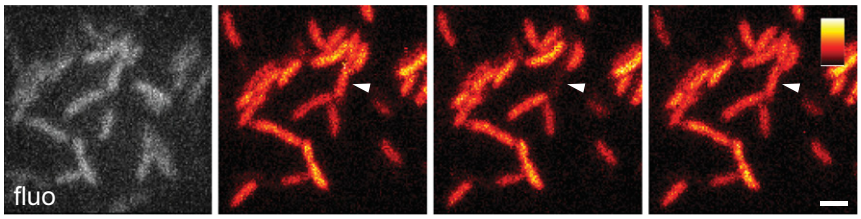

Fig. S7. Blinking of kanamycin-treated *E. coli* cells. *E. coli* Top10 cells expressing *ilux* were imaged under an LB agar pad containing 50 μg/mL ampicillin and 100 μg/mL kanamycin. Single images were taken with 3-min exposure time. The blinking of a cell in three consecutive images is indicated. A fluorescence (fluo) image excited with a 405-nm laser is shown in gray. The same color map was used for all bioluminescence images. (Scale bar: 2 μm.)

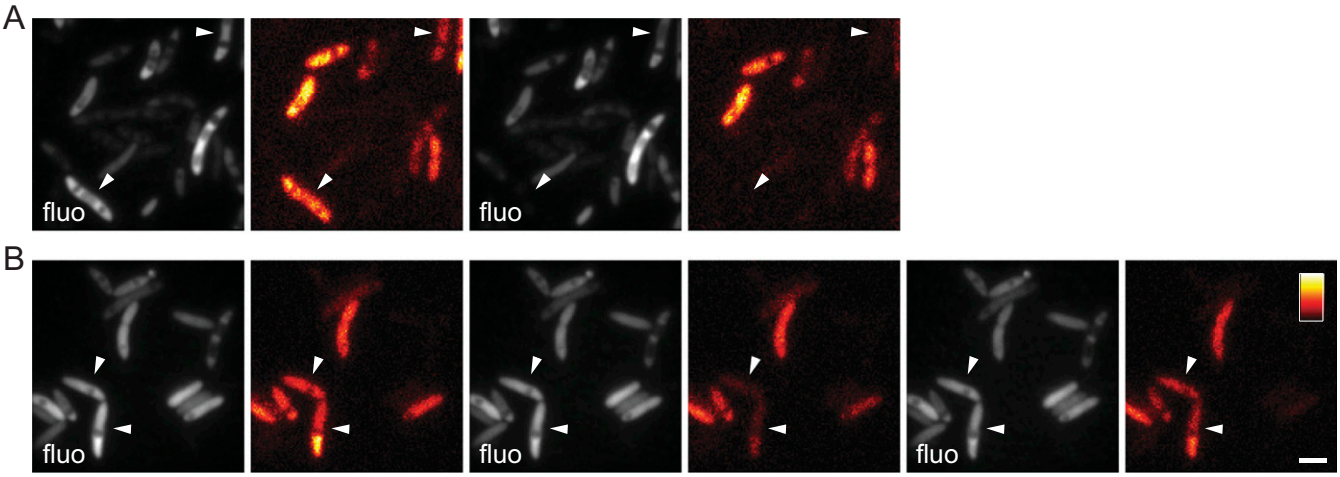

Fig. S8. Fluorescence (fluo) of *luxB*-EYFP in kanamycin-treated *E. coli* cells. *E. coli* Top10 cells expressing *ilux* with EYFP-tagged *luxB* were imaged under an LB agar pad containing 50 μg/mL ampicillin and 100 μg/mL kanamycin with exposure times of 10 min. Fluo images of EYFP excited with a 491-nm laser were taken between the bioluminescence images and are shown in gray. (*A*) Some cells with irreversible loss of bioluminescence retained EYFP fluo, whereas other cells lost EYFP fluo. (*B*) In blinking cells, EYFP fluo was fully preserved. The same color map was used for all fluo and bioluminescence images in each row. (Scale bar: 2 μm.)

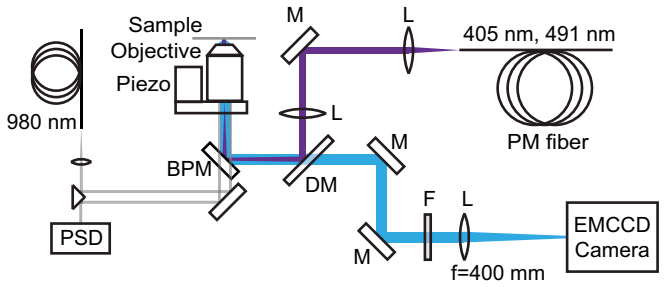

Fig. S9. Schematic setup of the microscope. Bioluminescence was collected by an oil immersion objective lens and directed to an electron multiplying charge-coupled device (EMCCD) camera using dielectric mirrors [back side-polished dielectric mirror (BPM) and mirror (M)] optimized for the visible wavelength range. The light was spectrally filtered by a short-pass filter (F) and focused onto the camera using a lens (L) with a focal length of 400 mm. For focusing and selection of cells, a wide-field excitation with 405 nm and 491 nm was implemented. Both lasers were coupled into the setup through a polarization-maintaining (PM) optical fiber. A dielectric mirror (DM) was used to separate the excitation light from fluorescence. Long-term stability of the focus position was provided by a custom-built focus lock system. This was based on the detection of a TIR signal using a position-sensitive diode (PSD) and repositioning the objective lens with a *z* piezo. In- and outcoupling of the 980-nm light for the focus lock was achieved through a BPM.

Table S1. Primers used for cloning and error-prone PCRs

Primer name	Sequence
pGEX(–) BamHI fwd	CAGGGGCCCCTGGGATCCCCGGAATTCCCG
pGEX(–)BamHI rev	TATAGGGGACATGGATCCTGTTTCCTGTGT
pQE(–) BamHI fwd	CGTAATGGATCCGCATGCGAGCTCG
pQE(–) BamHI rev	GTTCAGGGATCCAGTTAATTTCTCCTCTTTAATGAATTCTGTGT
luxC BamHI fwd	TTAGATGGATCCATGACTAAAAAAATTTCA
luxE SalI rev	TCTTAGGTCGACTCAACTATCAAACGCTTC
fre SalI fwd	GTAACTGTCGACCTAAGGAGAAAGAAATGACCACACTGAGC
fre NotI rev	TCAATGGCGGCCGCTTAGATAAATGCGAAG
frp SalI fwd	GTAACTGTCGACCTAAGGAGAAAGAAATGGTGAAGATACAG
frp NotI rev	CTTAGAGCGGCCGCTTACCTTTTGGCAAGGC
luxA SalI fwd	GTAACTGTCGACCTAAGGAGAAAGAAATGAAATTTGGAAACTTTTTGC
luxA NotI rev	GTAAGTGCGGCCGCCTAATATAATAGCGAACGTTGTT
luxB NotI rev	CTTAGAGCGGCCGCTTAGGTATATTCCATGTGGTAC
luxC SalI fwd	GTAACTGTCGACCTAAGGAGAAAGAAATGACTAAAAAAATTTCATTCATTATTAACG
luxD NotI rev	CTTAGAGCGGCCGCTTAAGACAGAGAAATTGCTTG
luxE SalI fwd	GTAACTGTCGACCTAAGGAGAAAGAAATGACTTCATATGTTG
luxE NotI rev	CTTAGAGCGGCCGCTCAACTATCAAACGCTTC
luxA EcoRI fwd	TGTATCGAATTCATGAAATTTGGAAACTTTTTG
linker luxDA EcoRI rev	TGTATCGAATTCAGAGAGTCCTTATATTGCTAT
linker luxBE NcoI fwd	TGTATCCCATGGTAGATTTCGAGTTGCAGCGAG
luxB NcoI rev	TGTATCCCATGGTTAGGTATATTCCATGTGGTA
EP luxAB EcoRI fwd	GCAATATAAGGACTCTCTGAATTC
EP luxAB NcoI rev	GCTGCAACTCGAAATCTACCATGG
EP luxCD BamHI fwd	GGATAACAATTTCACACAGGAAACAGGATCC
EP luxCD EcoRI rev	TTTCATGAATTCAGAGAGTCCTTATATTGCTATTTGAGTG
EP luxE NcoI fwd	ACCTAACCATGGTAGATTTCGAGTTGCAGC
EP luxE SalI rev	GCGGCCGCTCGAGTCGAC
EYFP EcoRI fwd	GCGGAATTCATGGTGAGCAAGGGCGAGGA
EYFP overlap luxA rev	CCAAATTTCATGCTGCCCTTGTACAGCTCGTCCAT
luxA overlap EYFP fwd	GTACAAGGGCAGCATGAAATTTGGAAACTTT
luxA overlap luxA-EYFP rev	CTCGCCCTTGCTCACCATGCTGCCATATAATAGCGAACGTTGTTT
EYFP fwd	ATGGTGAGCAAGGGCGAG
EYFP rev	CTTGTACAGCTCGTCCAT
luxB overlap luxA-EYFP fwd	GGCATGGACGAGCTGTACAAGTAGCTAAGGAGAAAGAAATGAAATTTGGATTGTTCTTCC
luxA overlap EYFP-luxB rev	CTCGCCCTTGCTCACCATTTCTTTCTCCTTAGCTAATATAATAGCGAACGTTGTTT
luxB overlap EYFP-luxB fwd	GGCATGGACGAGCTGTACAAGGGCAGCATGAAATTTGGATTGTTCTTCC
luxB overlap EYFP rev	CTCGCCCTTGCTCACCATGCTGCCGGTATATTCCATGTGGTACTTC
EYFP NcoI rev	AATCTACCATGGCTACTTGTACAGCTCGTCCAT
luxB-His NcoI rev	CTGAAGACCATGGTTAGTGATGGTGATGGTGATGGCTGCCGGTATATTCCATGTGGTACTTC
His-luxC BamHI fwd	TAAGTAGGATCCATGCATCACCATCACCATCACGGCAGCATGACTAAAAAAATTTCATTC
luxD-His EcoRI rev	TATGAATTCAGAGAGTCCTTATATTGCTATTTGAGTGATAGAATATCTCAATAGATT-TTAGTGATGGTGATGGTGATGGCTGCCAGACAGAGAAATTGCTTGATTTTC
luxE-His SalI rev	AGCAACGTCGACTCAGTGATGGTGATGGTGATGGCTGCCACTATCAAACGCTTCGGT
His-frp SalI fwd	CTTCGTGTCGACCTAAGGAGAAAGAAATGCATCACCATCACCATCACGGCA-GCATGGTGAAGATACAGCCC
ifrp NotI rev	GTTGATGCGGCCGCTTACCTTCTGGCAAGGCC
frp-His NotI rev	CTGAAGAGCGGCCGCTTAGTGATGGTGATGGTGATGGCTGCCCCTTTTGGCAAGGCCCTT
ifrp-His NotI rev	CTGAAGAGCGGCCGCTTAGTGATGGTGATGGTGATGGCTGCCCCTTCTGGCAAGGCCCTT
luxA overlap luxA-His rev	GTGATGGTGATGGTGATGGCTGCCATATAATAGCGAACGTTGTTTTTCT
luxB overlap luxA-His fwd	AGCCATCACCATCACCATCACTAGCTAAGGAGAAAGAAATGAAATTTGG
luxC overlap luxC-His rev	GTGATGGTGATGGTGATGGCTGCCTGGGACAAATACAAGGAACTTATC
luxD overlap luxC-His fwd	GCCATCACCATCACCATCACTAATAGGTAAAAAGTATGGAAAATGAATC
FLuc BamHI fwd	GTTATGGGATCCATGGAAGATGCCAAAAAC
FLuc SalI rev	CGTTGAGTCGACCTAGACGGCGATCTTGCCGCC
frp XmaI NotI rev	CTTCATGCGGCCGCTATCCACCCGGGTTCTTTCTCCTTAGTTACCTTCTGGCAAGGCCC
KanR SpeI fwd	GTTGATACTAGTATGAGCCATATTCAACGG
KanR AscI rev	GTTGATGGCGCGCCTTAGAAAAACTCATCGAG
pQE(–) AscI fwd	GTTGATACTAGTACTCTTCCTTTTTCAATATTATTGA
pQE(–) SpeI rev	GTTGATGGCGCGCCCTGTCAGACCAAGTTTACTCATAT
frp AscI XmaI NotI rev	CGCAAGAGCGGCCGCTATCCACCCGGGCTAGAAGGCGCGCCACTTTTTAC-CTATTACCTTCTGGCAAGGCC
QUEEN-2m AscI fwd	GCATCTGGCGCGCCATGAAAACTGTGAAAGTG
QUEEN-2m XmaI rev	TCAAGTCCCGGGTCACTTCATTTCCGCA

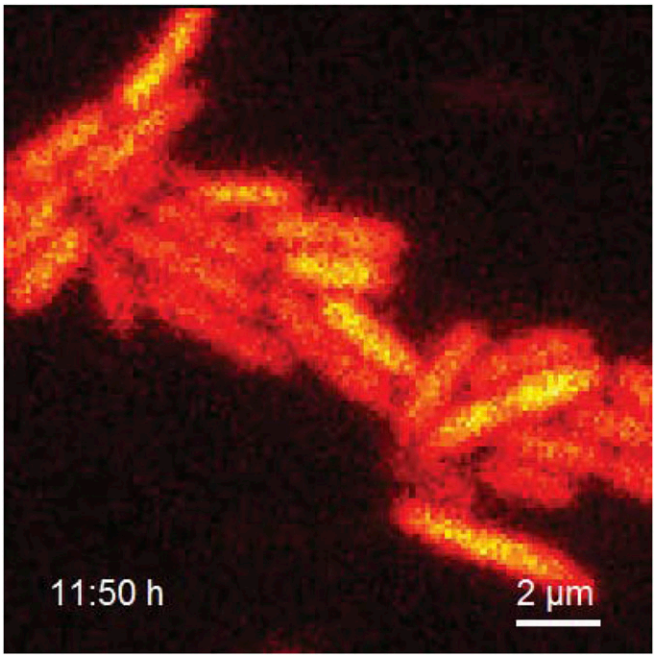

Movie S1. Cell division of *E. coli* Top10 cells expressing *ilux*. *E. coli* Top10 cells expressing *ilux* were imaged under an LB agar pad containing 50 μg/mL ampicillin. Single images were taken with 10-min exposure time. (Scale bar: 2 μm.)

Movie S1

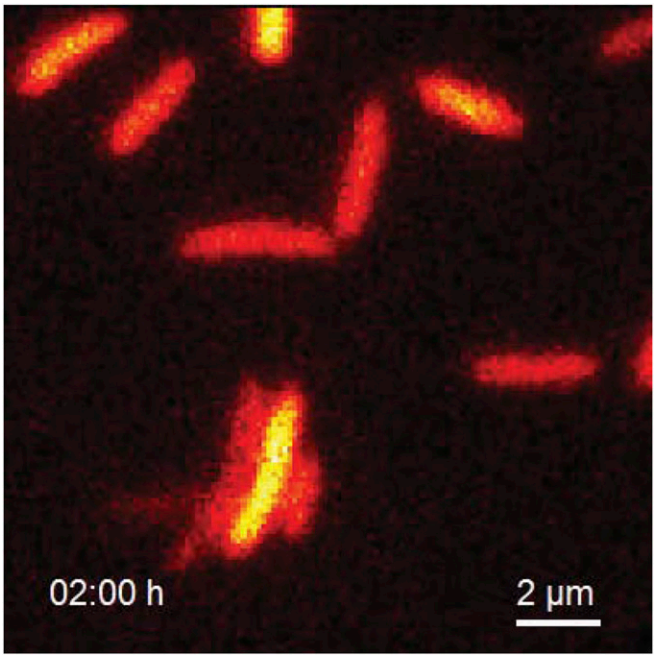

Movie S2. *E. coli* Top10 cells expressing *ilux* in the presence of timentin. *E. coli* Top10 cells expressing *ilux* were imaged under an LB agar pad containing 50 μg/mL ampicillin and 100 μg/mL timentin. Single images were taken with 10-min exposure time. (Scale bar: 2 μm.)

Movie S2

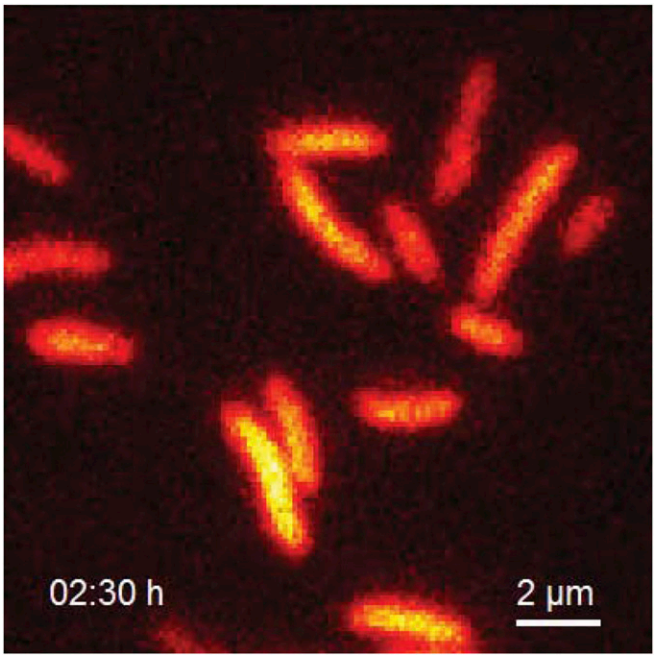

Movie S3. *E. coli* Top10 cells expressing *ilux* in the presence of kanamycin. *E. coli* Top10 cells expressing *ilux* were imaged under an LB agar pad containing 50 μg/mL ampicillin and 100 μg/mL kanamycin. Single images were taken with 10-min exposure time. (Scale bar: 2 μm.)

Movie S3

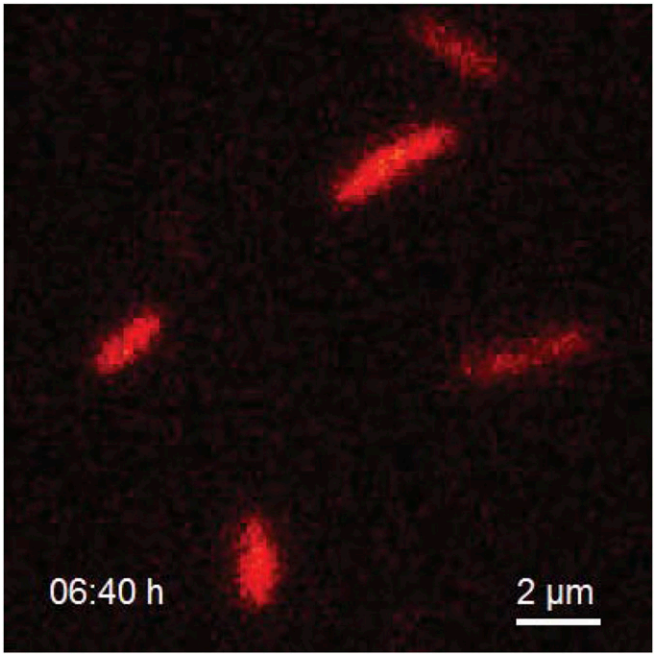

Movie S4. "Blinking" of *E. coli* Top10 cells expressing *ilux* in the presence of kanamycin. *E. coli* Top10 cells expressing *ilux* were imaged under an LB agar pad containing 50 μg/mL ampicillin and 100 μg/mL kanamycin. Single images were taken with 10-min exposure time. (Scale bar: 2 μm.)

Movie S4

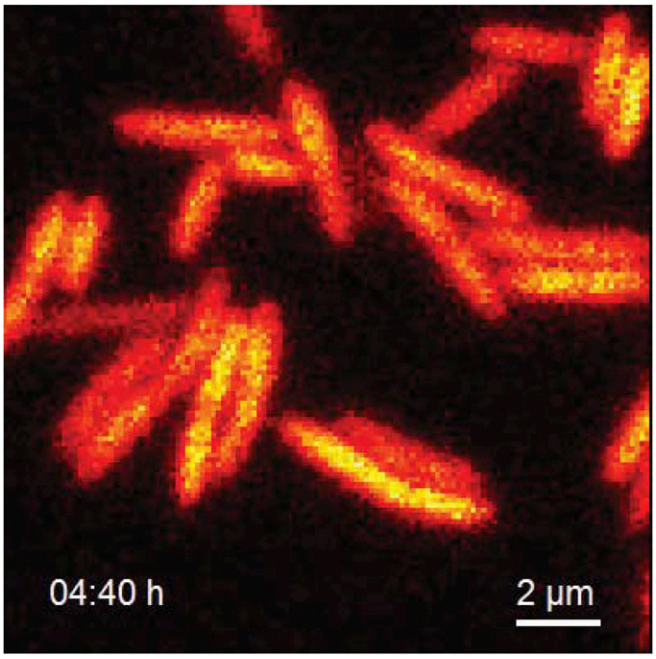

Movie S5. Kanamycin-resistant *E. coli* Top10 cells expressing *ilux* in the presence of kanamycin. *E. coli* Top10 cells expressing *ilux* from pQE(–) containing a kanamycin instead of ampicillin resistance marker were imaged under an LB agar pad containing 100 μg/mL kanamycin. Single images were taken with 10-min exposure time. (Scale bar: 2 μm.)

Movie S5